ANALYSIS OF DEFORMATIONAL TRANSFORMATIONS WITH SPATIO-TEMPORAL CONTINUOUS WAVELET TRANSFORMS. *

Jonathan Corbett *, *Jean-Pierre Leduc* *, *Mingqi Kong* †

Washington University in Saint Louis
* Department of Mathematics
† Department of Systems Science and Mathematics
One Brookings Drive, P.O. Box 1146
Saint Louis, MO 63130

ABSTRACT

This paper deals with the estimation of deformational parameters in discrete spatio-temporal signals. The parameters of concern correspond to time-varying scales. As such, they can be the coefficients of either a Taylor expansion of the scale or a given deformational transformation. At first sight, there are just a few deformational transformations that provide continuous wavelet transforms. The approach presented in this paper associates deformational transformations to motion transformations taking place in higher dimensional spaces and projected on the sensor plane. Then, finding continuous wavelet transforms becomes much easier since numerous continuous wavelet transforms have already been defined for motion analysis. It is also known that spatio-temporal continuous wavelet transforms provide minimum-mean-squared-error estimates of motion parameters. Any deformational transformation of features embedded in a spatio-temporal signal may always be related to the projection on the sensor plane of the motion of a rigid object taking place in a higher dimensional space. This reasoning applies conversely. The associated rigid motion may be actual or virtual, may take place either on a flat space or on a curved space immersed in higher dimensions. Continuous wavelet transforms for the estimation of deformational parameters may be then deduced from those already existing in motion analysis.

1. INTRODUCTION

The continuous wavelet transforms are defined as a linear mapping $W_\Psi : \Psi \rightarrow [W_\Psi\ s](g) = <\Psi_g|s>$ where $< .|. >$ is an inner product between the continuous wavelets Ψ_g and the signal s. Moreover the wavelet transform W_Ψ is an isometry from $L^2(\mathbf{R}^n, d\vec{x})$ to $L^2(G, dg)$. In this paper, the spatio-temporal signal $s(\vec{x}, t)$ belongs to $L^2(\mathbf{R}^n \times \mathbf{R}, d\vec{x}dt)$. The continuous wavelets, $\Psi_g(\vec{x}, t)$, are unitary irreducible square-integrable representations of a Lie group G and $g \in G$.

Continuous wavelet transforms have already been successfully applied to analyze motion in digital image sequences. *Motion analysis* [1] means motion detection, parameter estimation, tracking, classification and selective reconstruction. *Parameter estimation* consists in estimating the actual position, velocity, and accelerations (translational and/or angular motion) of moving objects in digital signal. It has been shown recently that continuous wavelet transforms discretized for digital signal processing perform *minimum-mean-squared error estimations* [5] of the motion parameters as they appear within the digital signal. Square-integrable representations of Lie group have important properties that support perfect reconstruction, de-noising application, sampling and interpolation through reproducing kernel. If the group representations fail to meet square-integrability, they loose the properties and behave as matched filters (i.e. as correlators).

The existence of specific continuous wavelet transforms each with specific conditions of admissibility have already been associated to specific motion transformations. These continuous wavelet transforms refer to the analysis of motions on flat space or motion on manifolds. Motion on flat space can be translational (constant velocity [5, 6], and accelerated [8]), or rotational (angular velocity and angular accelerations [9]). Motion on manifolds refers to motion on surface of either constant curvatures (spheres and hyperboloids) or variable curvature embedded in $\mathbf{R}^n \times \mathbf{R}$ [10]. The analysis may be performed according to different spatial and time scales. Another related issue is the estimation of actual motion taking place in the $\mathbf{R}^3$ field of observation instead of estimating the captured motion. To yield actual estimations, it is assumed that the initial mechanical conditions are known in terms of position, surface, velocity,... In the most basic case of estimating instantaneous velocity, the relative position of the object and the sensor will suffice. The solution of this problem is intimately related to the estimation of deformation captured on the sensor plane. This is the topic to be developed in the sequel.

In this paper, we extend the previous work described here above to develop continuous wavelets that analyze deformational transformations in spatio-temporal signals. Only digital image sequences captured from planar sensor are taken as simulation examples but this theory extends in extenso to deal with complex signals for radar and sonar applications. Deformational transformations and motions in higher dimensional space are related to each other. These two kinds of transformation may be described as follows. First, the deformations observed in a captured scene originate from the motion of a rigid object taking place in a three or higher multi-dimensional space that is eventually projected on the plane of the sensor. The meaning of the projection has still to be defined. In the case at hand, the component of the velocity orthogonal to the sensor plane is not captured as a velocity but instead as a deformational transformation involving a change of scale. Second, any real deformation may be described as a pure transformation of the plane like the conformal mapping. In fact, any real deformation may also be considered as originating from the motion of a rigid object taking place in some higher dimensions and projected on the sensor. This sensor may be any kind of surface and

*The authors want to thank Prof. B. K. Ghosh of the Department of Systems Science and Mathematics who provided the numerical computation support to this work.

basically a plane. The motion may moreover take place on a flat space or on a manifold. In addition, several kinds of projections may be considered (homothety, orthogonal projection, stereographic projection). The solution to this problem is therefore not unique. This paper provides an introduction to this huge topic.

The paper is structured as follows. First, it outlines some of the spatio-temporal continuous wavelets. Though initially developed for motion-analysis purpose, these wavelets can be of prime interest for deformational-parameter estimation. To demonstrate this proposition, the following section explains how a deformation may be interpretated as a projected motion leading to the actual concept of *deformational motion*. The motion takes place in higher dimensions and is not univocally defined. The projection operation is not imposed and may be orthogonal, stereographic,... An opposite approach consists in investigating some deformations and defining the motions that are related. Eventually, simulation results are presented that analyze motion on an horizontal plane.

2. MOTION ANALYSIS

Several continuous wavelet transforms have already been defined to analyze motion. In this section, we address three different kinds of motion based continuous wavelet transforms that can be exploited to estimate deformational parameters in the next section.

The Galilean wavelets are representations of the Galilei group G that describe velocity-based spatio-temporal transformations. The group is defined with the following set of parameters $g = \{g \in G | g = (\phi, \vec{b}, \tau, \vec{v}, a, R)\}$ where $\vec{b} \in \mathbf{R}^n$ and $\tau \in \mathbf{R}$ are the spatial and the temporal translations respectively, $\vec{v}$ the velocity, a the scale, and $R \in SO(n)$ the spatial orientation. ϕ is the parameter of the central extension of the group. The unitary and irreducible group representations in the spatio-temporal Hilbert space $L^2(\mathbf{R}^n \times \mathbf{R}, d\vec{x}dt)$ of the signal read [6] in this case

$$\left[T(g)\hat{\Psi}\right](m_1, \vec{k}, \omega) = a^{\frac{n+2}{2}} e^{i(m_1\phi + \omega\tau + \vec{k}\cdot\vec{b})} \hat{\Psi}\left(m_1', \vec{k}', \omega'\right) \tag{1}$$

with

$$\vec{k}' = aR(-\theta_0)[\vec{k} + m_1\vec{v}],\ \omega' = \omega + \vec{k}\cdot\vec{v} + \frac{1}{2}m_1\vec{v}^2,\ m_1' = a^2 m_1 \tag{2}$$

The variables m, $\vec{k}$ and ω are Fourier variables corresponding to the parameters ϕ, $\vec{b}$, and τ. The symbol $\cdot$ stand for the scalar product. The existence of these wavelets is provided by an admissibility condition presented in [6].

The accelerated wavelets are representations of another Lie group G built with the following parameters $G = \{g \in G | g = (\phi_2, \phi_3, \vec{b}, \tau^2, \vec{\gamma}, a, R)\}$ where $\vec{\gamma} \in \mathbf{R}^n$ and $\tau^2 \in \mathbf{R}$ stand for the first order of acceleration and the squared temporal translation respectively. ϕ_2 and ϕ_3 both define the central extension. The unitary irreducible representations read [8]

$$\begin{aligned}[\widehat{T}(g)\widehat{\Psi}]&\left(m_i, \vec{k}, \omega, \sigma\right) \\ &= a^{\frac{n+2}{2}} e^{i(m_2\phi_2 + m_3\phi_3 + \vec{k}\cdot\vec{b} + \omega\tau + \sigma\tau^2)} \widehat{\Psi}\left(m_i', \vec{k}', \omega', \sigma'\right)\end{aligned} \tag{3}$$

$$\begin{array}{ll} \vec{k}' = aR^{-1}(\vec{k} + m_3\vec{\gamma}_0), & \omega' = \omega + \vec{v}\cdot\vec{k} + \frac{1}{2}m_2\vec{\gamma}_0^2, \\ \sigma' = \sigma + \frac{1}{2}\vec{k}\cdot\vec{\gamma}_0 + \frac{1}{2}m_3\vec{\gamma}_0^2, & m_i' = a^2 m_i, \quad i = 2, 3. \end{array} \tag{4}$$

The existence of these wavelets is provided by an admissibility condition similar to that one obtained for the Galilean wavelets [8].

The wavelets on manifolds are representations of Lie group G built with the following parameters $g = \{\Phi, \vec{p}, \tau, \vec{v}, A, R_0\}$ where $\vec{p}$ is a generalized spatial translation on the manifold, τ the temporal translation, $A \in \mathbf{R}^{n^2}$ the spatial matrix scale, $\Phi \in \mathbf{R}^{n^2}$ the matrix central extension and R_0 the spatial orientation. The unitary and irreducible representations at point $\vec{p}_0$ on the surface read [10] in this case

$$[\widehat{T_{\vec{p}_0}}(g)\widehat{\Psi}](\vec{k}, \omega, M) = \lambda^{1/2} e^{i[tr(M\Phi) + \omega\tau + <\vec{k}|\vec{p}>]} \widehat{\Psi}\left(\vec{k}', \omega', M'\right) \tag{5}$$

where $\lambda = |\det\left[A^3(\Gamma_{p_0 v} + I)(B_{p_0} + I)\right]|$, and

$$\vec{k}' = R_0^T A^T [B_{p_0} + I]^T [\Gamma_{p_0 v} + I]^T \vec{k} \tag{6}$$

$$\omega' = \omega \tag{7}$$

$$M' = R_0^{2\ T} A^{2\ T} M \tag{8}$$

where $[B_{p_0} + I]$ and $[\Gamma_{p_0 v} + I]$ stand as matrix transformations taking place on the manifold and depending respectively on the translation $\vec{p}$ and both the translation $\vec{p}$ and boost $\vec{v}$. To stress on the difference with the flat space approach, the scalar/inner product is denoted here as $<\vec{k}|\vec{p}> = g_{ij}k^i p^j$ where g_{ij} is the intrinsic metric associated to the manifold $\mathbf{M}$ embedded in $\mathbf{R}^n$. The symbol tr stands for the matrix trace. In the next section, these wavelet transforms are going to be projected from $\mathbf{R}^3 \times \mathbf{R}$ onto the sensor plane $\mathbf{R}^2 \times \mathbf{R}$ to provide estimations of deformation parameters.

3. DEFORMATIONS AS PROJECTED MOTION

In this section, we analyze the projections of motion on the sensor plane and associate them with deformational transformations. The usual projection that take place within the cone of sensor visibility (Figure 1) is a homothety (i.e. a scaling). If the depth of the object is negligible in comparison to the object-to-sensor distance, the projection may be obtained as an orthogonal projection composed with a scaling.

The motion captured in the sensor plane is obtained after a projection on planes Π_0, Π_1, Π_2 parallel to sensor at time $\tau = 0,\ 1,\ 2$ and a homothety that rescales the projection down to the plane of the sensor Figure 1. Let us denote W the width of the rigid object and S_0 the size of the object captured by the camera. Let us also denote d the distance between the summit of the cone of sensor visibility and the plane Π_0 of the starting location. It is fairly reasonable to assume that the depth δ of the object is small or negligible. The scale $a_0 = \frac{W}{S_0}$ is observed from plane Π_0 at time $\tau = 0$. At time $\tau = n$, the size perceived from plane Π_n by the camera is given by $a_n = \frac{W}{S_n} = \frac{W}{S_0(1 - \frac{v_z}{d}\tau)} = \frac{a_0}{1 - \frac{v_z}{d}\tau} = a_0\ [1 + \frac{v_z}{d}\tau + (\frac{v_z}{d})^2\tau^2 + \ldots] = a_0[1 + a_1\tau + a_2\tau^2 + \ldots + a_n\tau^n + \ldots]$. The series is convergent while $|\frac{v_z}{d}\tau| < 1$ and this corresponds to the physical nature of the observation. Let us construct the referential of the embedding space $\mathbf{R}^3$ such that axis x and axis y ar orthogonal and coincide with the sensor plane and axis z is orthogonal to the sensor plane. Therefore, the components V_{Tx} and V_{Ty} of the total velocity are captured in the signal up to a multiplicative constant. The orthogonal component V_{Tz} has to be estimated from $a_0,\ a_1, \ldots, a_n$ as a rate of expansion $\frac{v_z}{d}$. The Fourier transform (denoted $\widehat{\ }$) of the projected signal and that of the original signal are denoted $\widehat{S}_p(\vec{k}, \omega)$

and $\widehat{S}(\vec{k},\omega)$ respectively. Let us then consider $S(\vec{x},t)$ and the projected version $S_P(\vec{x},t) = S(\frac{a_0}{1-\frac{v_z}{d}t}\vec{x})$. Then, the Fourier transform reads then $(n=2)$

$$\begin{aligned}
S_P(\vec{k},\omega) &= \int_{\mathbf{R}^n}\int_{\mathbf{X}_t} S\left(\frac{a_0}{1-\frac{v_z}{d}t}\vec{x}\right) e^{-i(\vec{k}\cdot\vec{x}+\omega t)}\, d\vec{x}dt \\
&= \int_{\mathbf{R}^n}\int_{\mathbf{X}_t} S(\vec{x}\,')e^{-i(\frac{1-\frac{v_z}{d}t}{a_0}\vec{k}\cdot\vec{x}+\omega t)}\ \frac{1-\frac{v_z}{d}t}{a_0}d\vec{x}\,'dt \\
&= \int_{\mathbf{X}_t} \widehat{S}_k(\frac{1-\frac{v_z}{d}t}{a_0}\vec{k})e^{-i\ \omega t}\ \frac{1-\frac{v_z}{d}t}{a_0}dt \\
&= \int_{\mathbf{X}_t} \Pi(\frac{v_z}{d})\widehat{S}^k\left(\vec{k},t\right)e^{-i\ \omega t}\ \frac{1-\frac{v_z}{d}t}{a_0}dt \\
&= \frac{1}{a_0}\left[1-i\frac{v_z}{d}\frac{\partial}{\partial\omega}\right]\widehat{\Pi}(\frac{v_z}{d})\widehat{S}(\vec{k},\omega) \qquad (9)
\end{aligned}$$

with $\mathbf{X}_t = [0,\frac{d}{v_z})$ and $\Pi(\frac{v_z}{d})\widehat{S}^k\left(\vec{k},t\right) = \widehat{S}^k\left(\frac{1-\frac{v_z}{d}t}{a_0}\vec{k}\right)$.

The group representations are defined in the Fourier domain that has to be related to the projection on the sensor planes. It easy to see according to the assumptions made in the previous paragraph that the projection of the signal on the sensor plane may be obtained using the slice-projection Fourier theorem [2] restated for this application and spatio-temporal signals. According to this theorem, the Fourier transform $S_{p_R}(\vec{k}\,',\omega)$ of the projection $S_{p_R}(\vec{x}\,',t)$ of the signal $S(\vec{x},t)$ with $\vec{x}\in\mathbf{R}^n$ taken at an angle $R\in SO(n)$ is the $(n-1)$-dimensional Fourier transform of the signal evaluated on a plane at origin oriented at angle R. This cross-sectional Fourier transform is the slice at angle R of $S(\vec{k},\omega)$ the n-dimensional Fourier transform of $S(\vec{x},t)$. Then, the spatio-temporal projection of the signal is given by

$$S_{p_R}(\vec{x}^{'},t) \;=\; \int_{\mathbf{R}^n} S(\vec{x},t)\delta(\vec{n}.\vec{r}-d)d\vec{x} \qquad (10)$$

The Fourier transform of the projection reads after a change of variable [2]

$$\widehat{S}_{p_R}(\vec{k}\,',\omega) \;=\; \widehat{S}_p(R\vec{k},\omega) \qquad (11)$$

In our application, the section is 2-dimensional on the spatial frequencies and one-dimensional on the temporal frequency The section is taken in the representations of the Galilean wavelet defined in the dual Fourier space $(\mathbf{R}^3\times\mathbf{R})$ and rescaled according to Equation (9). As a section of a square integrable representation, the new representation is still square integrable and then an analyzing wavelet.

The scale varies frame-per-frame as $a_n = a_0\frac{1}{1-\frac{v_z}{d}\tau}$; $\tau = n$. The estimation of the parameter v_z is derived from as a classical tracking problem of velocity $\vec{v}\in\mathbf{R}^3$ by searching the local maximum of the square modulus of the wavelet transform as follows [5]

$$\vec{v}_* \;=\; \arg\max_{\vec{v}} \left|< \Psi^p_{\vec{b}_0,\tau_0,\vec{v}_0,a_0,R_0}|s>\right|^2 db_x\ db_y; \qquad (12)$$

with the Galilean group: $g = \{\vec{b},\tau,\vec{v},a,R\}$ in $\mathbf{R}^3\times\mathbf{R}$ and Ψ^p the projected wavelet.

So far v_z has been supposed constant in time. In case of an accelerated motion, several parameters v_z, and γ_z's have to be estimated successively starting with the velocity $\vec{v}\in\mathbf{R}^3$ and proceeding towards several order of acceleration $\vec{\gamma}\in\mathbf{R}^3$ [8]. In case of a motion on a sphere, the evolution of $v_z(t)$ is known from the angular velocity $\vec{\rho}$ and the object-to-sensor distance $\vec{d}$. Therefore, $\vec{v} = \vec{\rho}\times\vec{d}$, where $\times$ is the vector product, determines $v_z = f(v_x,v_y;t)$.

4. MOTION ASSOCIATED TO DEFORMATION

In this section, we proceed in a converse way to examine examples of virtual motion associated to planar deformations. The most simple example of deformation is the exponential expansion/contraction

$$s(\vec{x},t) \;=\; f(\exp[-(a_0+a_1t)]\vec{x},t) \qquad (13)$$

This case is amenable to Lie group analysis, representation and wavelets with or without the linearization of Mellin Transforms. This case will be presented in full range at the conference.

Another deformational transformation to be considered extends the previous exponential deformations into complex functional spaces. This is a unitary transformation $\vec{x}' = \begin{pmatrix} cosh(\alpha\tau) & sinh(\alpha\tau) \\ sinh(\alpha\tau) & cosh(\alpha\tau)\end{pmatrix}\vec{x}$ which belongs to the group $SO(1,1)$ and is contained in the Iwasawa decomposition [3] of the group $G = SU(1,1)$. Indeed, $g\in G$; $g = \begin{pmatrix}\alpha & \beta \\ \bar{\beta} & \bar{\alpha}\end{pmatrix}$ with $|\alpha|^2-|\beta|^2 = 1$. The Iwasawa decomposition of G leads to $G = HAN$ with $H = U(1)$, $A = SO(1,1)$, $N \equiv \mathbf{R}$ Explicitly, $g = a(\theta)\epsilon b(\phi)c(x)$ with $a(\theta) = \begin{pmatrix}\exp[i\theta/2] & 0 \\ 0 & \exp[-i\theta/2]\end{pmatrix}$, $b(\phi) = \begin{pmatrix} cosh(\alpha) & sinh(\alpha) \\ sinh(\alpha) & cosh(\alpha)\end{pmatrix}$, $\epsilon = \pm 1$, and $c(x) = \begin{pmatrix} 1+ix & -ix \\ ix & 1-ix\end{pmatrix}$. Geometric considerations in this case lead to considering the isomorphism between the unit disk $\mathcal{D}$ in the complex plane and group coset $SU(1,1)/U(1)$ that represent an hyperbolic surface. They represent an orbit of the co-adjoint representation of $SU(1,1)$ that leads to construct the unitary irreducible representations [3]. Let us denote $\mathcal{F}_k = \{f(z)|z\in\mathcal{D}\}$ the Fock-Bargmann space of holomorphic functions inside the unit disk [4] fulfilling the square-integrability condition $< f|f >= ||f||^2 < \infty$ with respect to the inner product

$$< f_1|f_2 > = \int_{\mathcal{D}} f_1(z)\bar{f}_2(z)d\mu_k \text{ with } d\mu_k = \frac{2k-1}{\pi}(1-|z|^2)^{2k-2}d^2z \qquad (14)$$

It is not difficult to see that if $f(z) = \sum_0^\infty c_nz^n$ then $||f||^2 = \sum_{n=0}^\infty \frac{\Gamma(n+1)\Gamma(2k)}{\Gamma(n+2k)}|c_n|^2$ and the functions $f_n(z) = \sqrt{\frac{\Gamma(n+2k)}{\Gamma(n+1)\Gamma(2k)}}$ form an orthonormal basis of the Hilbert space $\mathcal{F}_k$. If we define the action of the operator $T(g)$, $g\in SU(1,1)$, as

$$T(g)f(z) \;=\; (\beta z+\bar{\alpha})^{-2k}f\left(\frac{\alpha z+\bar{\beta}}{\beta z+\bar{\alpha}}\right) \qquad (15)$$

It can be shown [4] that the operator determines unitary and irreducible representations. Representations are square integrable and are continuous wavelets that can anlyze complex signals under the transformation. The motion related to those representation is a motion on horocycles in the unit disk $\mathcal{D}$ (the Smith chart) isomorphic to a motion on a hyperboloid (Lobatcheskian motion) [4].

5. NUMERICAL RESULTS

The numerical application presented in this section deals with the estimation of parameter $\frac{v_z}{d}$. The computations have been performed with Galilean wavelets defined in $\mathbf{R}^3 \times \mathbf{R}$ and projected on the sensor plane as described in Sections 2 and 3. An anisotropic *Morlet wavelet* is admissible as a mother wavelet in the Galilean family. The wavelet $\Psi(\vec{x}, t)$ is first calculated in the space and time domain and projected so as to generate $\Psi(\frac{a_0}{1-\frac{v_z}{d}t}\vec{x}, t)$. The wavelet is then transformed to the Fourier domain where the inner product with the signal $S(\vec{k}, \omega)$, $< T(g)\Psi|s >$, is computed. Figure 2 displays a natural scene where two objects (car) are moving on a horizontal plane (road). Figure [3] displays the energy densities i.e. the square modulus of the wavelet transform as a function of the scale a_0 and the parameter $\frac{v_z}{d}$ (in inverse time units). Two optima have been detected and correspond to two moving objects. They are located at ($\frac{v_{z1}}{d} = 0.5s^{-1}$, $a_{01} = 2.6$) and ($\frac{v_{z2}}{d} = 0.38s^{-1}$, $a_{02} = 1.8$). If we assume that $d_1 = 40$ m for the foreground car and a rate of 25 images per second, then we can estimate the approaching velocity component at $v_{z1} = 72$ km/h. In this scene the camera is located on a car traveling in the opposite direction; v_{z1} is a relative velocity about twice that one of the observed car. For the background car, if we assume $d_2 = 50m$, then $v_{z2} = 68.4$ km/s. The a_0's are rescaled in terms of standard deviation on the image display, i.e. car 1 starts in image $\tau = 0$ with a diameter of about 16 pixel intervals.

6. CONCLUSIONS

This paper has outlined the main principles of a powerful method that supports the estimation of deformational parameters in spatio-temporal signals. It has shown how any features in deformation can be virtually or actually related to a rigid feature moving in a space of higher dimensions projected onto the sensor plane. The correspondence depends on the geometry. Indeed, a deformational motion may originate either from an accelerated motion taking place on a plane tilted with respect to the sensor plane or from an uniform motion taking place on a curved surface. These observations open the door to further research works. When a parametric deformation model is adopted to perform tracking in a digital scene, there exist motion-based spatio-temporal wavelet transforms that can be involved in the parameter estimation.

REFERENCES

[1.] A. Tekalp "Digital Video Processing", *Prentice-Hall, 1995.*

[2.] D. E. Dudgeon and R. M. Mersereau "Multidimensional Digital Signal Processing", *Prentice-Hall, 1984.*

[3.] W. A. Knapp "Representation Theory of Semisimple Groups: an overview based on examples", *Princeton Univ. Press, 1986.*

[4.] J. R. Klauder and B. Skagertam "Coherent States: Applications in Physics and Math. Physics", *World Scientific, 1985.*

[5.] J.-P. Leduc, F. Mujica, R. Murenzi, M. J. S. Smith "Spatio-Temporal Wavelet Transforms for motion tracking", *ICASSP-97, Munich, Germany, 20-24 April 1997, Vol. 4, pp. 3013-3017.*

[6.] J.-P. Leduc "Spatio-Temporal Wavelet Transforms for Digital Signal Analysis", *Signal Processing, Elsevier, Vol. 60 (1), pp. 23-41, July 1997.*

[7.] J.-P. Leduc "Spatio-Temporal Wavelet Transforms for Digital Signal Analysis", *Signal Processing, Elsevier, Vol. 60 (1), pp. 23-41, July 1997.*

[8.] J.-P. Leduc, J. Corbett, M. Kong, V. M. Wickerhauser, B. K. Ghosh "Accelerated Spatio-temporal Wavelet Transforms: an Iterative Trajectory Estimation", *Proceedings of ICASSP-98, Seattle, Vol. 5, May 1998, pp. 2777-2780.*

[9.] M. Kong, J.-P. Leduc, B. K. Ghosh, J. Corbett, V. M. Wickerhauser "Wavelet based Analysis of Rotational Motion in Digital Image Sequences", *Proceedings of ICASSP-98, Seattle, Vol. 5, May 1998, pp. 2781-2784.*

[10.] J.-P. Leduc and J. Corbett "Spatio-Temporal Continuous Wavelets for the Analysis of Motion on Manifolds", *To appear in the Proceedings of the IEEE-SP International Symposium on Time-Frequency and Time-Scale Analysis, Pittsburgh, 6-9 October 1998, 4 pp.*

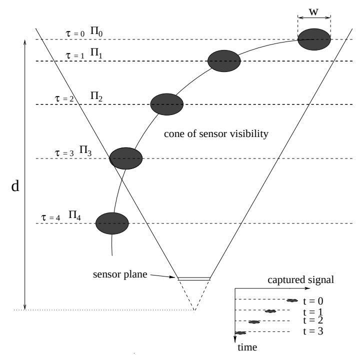

Figure 1. Projection on a rigid motion on the sensor plane.

Figure 2. The 20th image of the car digital image sequences.

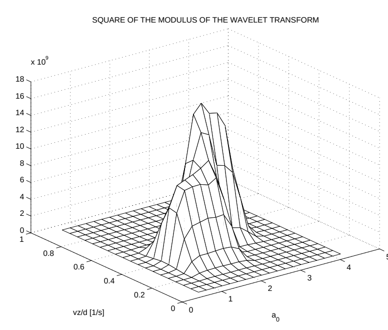

Figure 3. Estimation of the parameters $\frac{v_z}{d}$ and a, square modulus (energy) of the wavelet transform $| < T(g)\Psi|s > |^2 = F(a_0, \frac{v_z}{d})$ in the scene of Figure 2: two local maxima are displayed at ($\frac{v_{z1}}{d} = 0.5s^{-1}$, $a_{01} = 2.6$) and ($\frac{v_{z2}}{d} = 0.38s^{-1}$, $a_{02} = 1.8$) standing for the fore and back-ground car respectively. The estimations are based on a rate of 25 images per second.